

CHEMISTRY

A European Journal



Accepted Article

Title: Furanosyl oxocarbenium ion Conformational Energy Landscape maps as a tool to study the glycosylation stereoselectivity of 2-azidofuranoses, 2-fluorofuranoses and methyl furanosyl uronates

Authors: Stefan van der Vorm, Thomas Hansen, Erwin R. van Rijssel, Rolf Dekkers, Jerre M. Madern, Herman S. Overkleef, Dmitri V. Filippov, Gijsbert A. van der Marel, and Jeroen D. C. Codée

This manuscript has been accepted after peer review and appears as an Accepted Article online prior to editing, proofing, and formal publication of the final Version of Record (VoR). This work is currently citable by using the Digital Object Identifier (DOI) given below. The VoR will be published online in Early View as soon as possible and may be different to this Accepted Article as a result of editing. Readers should obtain the VoR from the journal website shown below when it is published to ensure accuracy of information. The authors are responsible for the content of this Accepted Article.

To be cited as: *Chem. Eur. J.* 10.1002/chem.201900651

Link to VoR: <http://dx.doi.org/10.1002/chem.201900651>

Supported by
ACES

WILEY-VCH

Furanosyl oxocarbenium ion Conformational Energy Landscape maps as a tool to study the glycosylation stereoselectivity of 2-azidofuranoses, 2-fluorofuranoses and methyl furanosyl uronates

Stefan van der Vorm, Thomas Hansen, Erwin R. van Rijssel, Rolf Dekkers, Jerre M. Madern, Herman S. Overkleef, Dmitri V. Filippov, Gijbert A. van der Marel and Jeroen D. C. Codée*

Abstract

The 3D shape of glycosyl oxocarbenium ions determines their stability and reactivity and the stereochemical course of S_N1 -reactions taking place on these reactive intermediates is dictated by the conformation of these species. The nature and configuration of functional groups on the carbohydrate ring effect the stability of glycosyl oxocarbenium ions and they control the overall shape of the cations. We here map the stereoelectronic substituent effects of the C2-azide, C2-fluoride and C4-carboxylic acid ester on the stability and reactivity of the complete suite of diastereoisomeric furanoses using a combined computational and experimental approach. Surprisingly all furanosyl donors studied react in a highly stereoselective manner to provide the 1,2-*cis* products, except for the reactions in the xylose series. The 1,2-*cis* selectivity in the *ribo*-, *arabino*- and *lyxo*-configured furanosides can be traced back to the lowest energy 3E or E_3 -conformers of the intermediate oxocarbenium ions. The lack of selectivity of the xylosyl donors is related to the occurrence of oxocarbenium ions, adopting other conformations.

Introduction

Stereoelectronic effects dictate the shape and behaviour of molecules. Understanding and harnessing these effects enables the conception of effective and stereoselective synthetic chemistry.^[1] Carbohydrates are densely decorated molecules bearing a variety of different functional groups in numerous configurational and stereochemical constellations.^[2,3] The decoration pattern of carbohydrates plays an all-important role in manipulations/transformations of the functional groups in the assembly of carbohydrate building blocks as well as in the union of two carbohydrates in a glycosylation reaction. During a glycosylation reaction a donor glycoside is generally activated to give an electrophilic species bearing significant oxocarbenium ion character.^[4] While steric effects are often decisive in determining the overall shape of a neutral molecule, in charged molecules electronic effects become more important and they may in fact outweigh steric effects. For example, protonated iminosugars, carbohydrates having the endocyclic oxygen replaced for a nitrogen, may change their conformation to place their ring substituents in a sterically unfavourable (*pseudo*)-axial orientation to stabilize the positive charge on the ring nitrogen.^[5-10] In line with these stereoelectronic effects, glycosyl donors that feature an “axial-rich” substitution pattern, are generally more reactive than glycosyl donors equipped with equatorially disposed functional groups.^[11-13] However, it is extremely

challenging to understand - let alone predict - what the overall effect of multiple ring substituents is on the reactivity of a particular glycosyl donor and as a result the effect on the stereoselectivity in a glycosylation reaction. Based on a computational strategy of Rhoad and co-workers,^[14] we have recently introduced a method to determine the conformational behaviour of furanosyl oxocarbenium ions.^[15–17] By calculating the relative energy of a large number of fixed furanosyl oxocarbenium ion conformers and mapping these in energy contour plots we could determine which conformations played an important role during furanosylation reactions and we were able to relate the population of the different conformational states to the stereoselectivity of the reactions. The introduced conformational energy landscape mapping method provided detailed insight into how the ring substituents - as stand-alone entities but also collectively - influenced the shape, stability and reactivity of the furanosyl oxocarbenium ions. In this initial study, only ether substituents were assessed. We here present an in-depth study on the stereoelectronic substituent effects of different functional groups that are all highly relevant in oligosaccharide synthesis. Understanding these effects will enable the development of effective glycosylation methodologies and aid in the interpretation of the outcome of glycosylation reactions. We have studied the effect of C2-fluoro and C2-azide substituents, as well as C4-carboxylic acid ester groups, as these functionalities are commonly employed in the assembly of fluorinated, *cis*-linked glycosamine containing or glycuronic acid featuring oligosaccharides, respectively.^[18–25]

Herein we describe the synthesis of a panel of twelve structurally varying furanosyl imidate donors, comprising all possible pentofuranosyl diastereoisomers (Figure 1, **1-12**), their glycosylation properties studied by experimental chemical glycosylations, as well as a computational investigation on the reactive intermediates active during the glycosylation and responsible for the stereoselective outcome of the reaction, the furanosyl oxocarbenium ion.

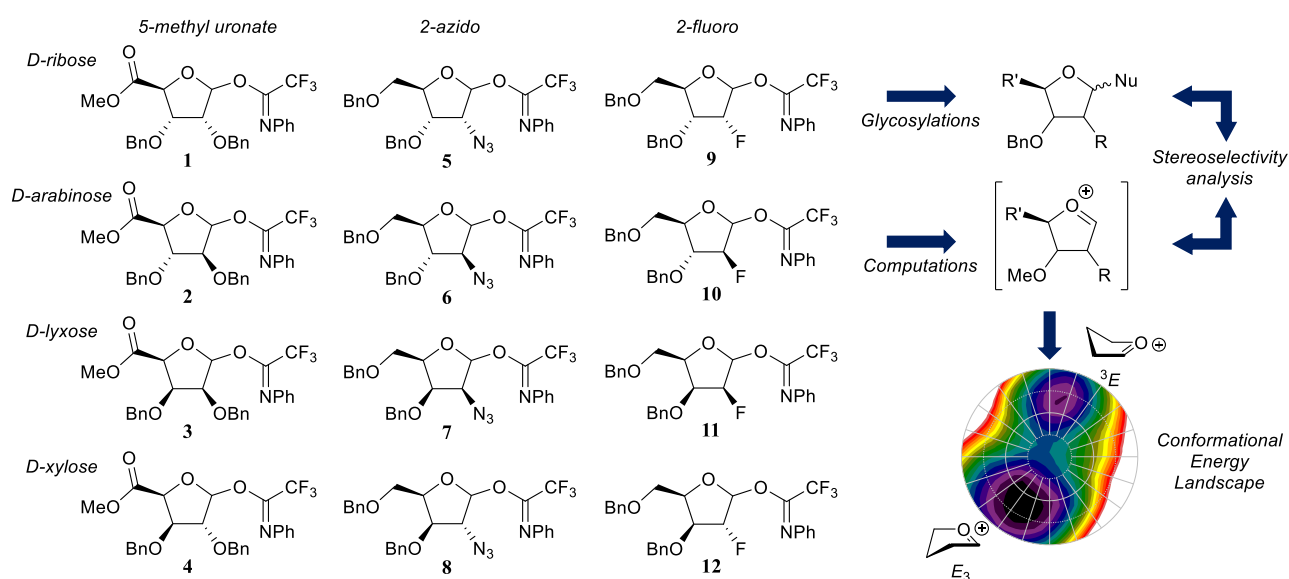


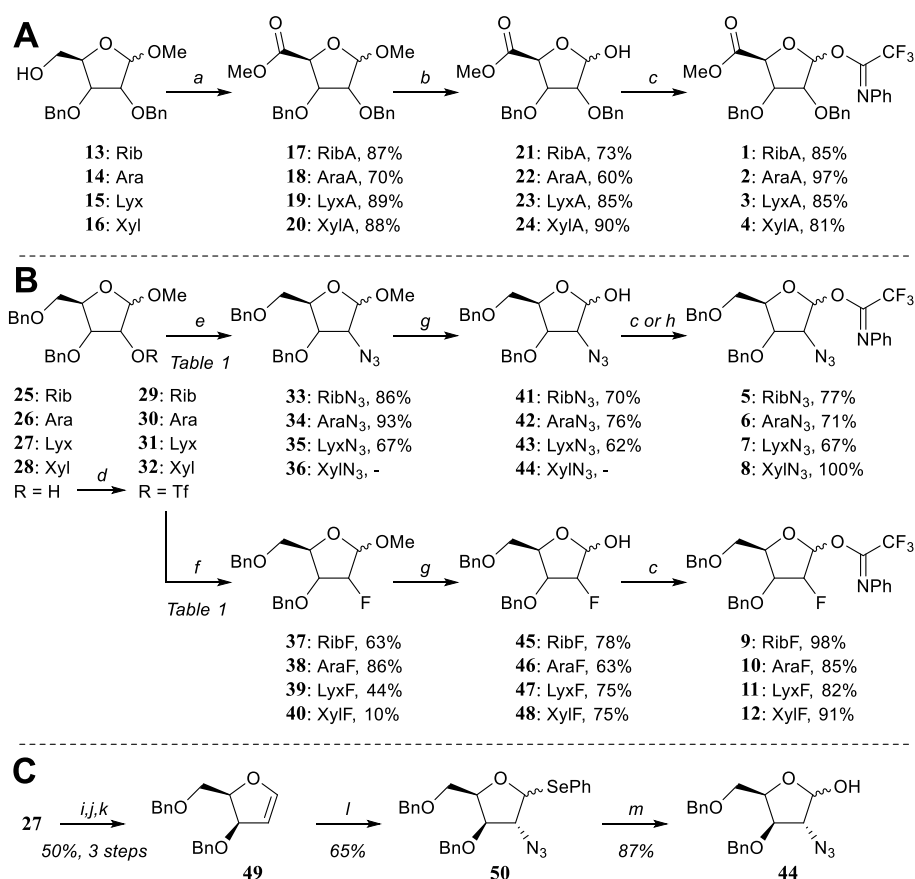
Figure 1. Target donors **1-12** and the subsequent stereoselectivity investigation by glycosylations and computational analysis.

Results and discussion

Synthesis

The set of *D-ribo-*, *D-arabino-*, *D-lyxo-* and *D-xyl-*configured furanosyl donors **1-12** (Figure 1) that was needed for this study was prepared as depicted in Scheme 1. All donors studied here were equipped with an *N*-phenyl trifluoroacetimidate anomeric leaving group.^[26] The uronic acid methyl esters **17-20** were obtained from their parent methyl furanosides **13-16**^[27-30] by a straightforward TEMPO/BAIB oxidation procedure of the primary alcohols, followed by methylation with MeI and K₂CO₃ (Scheme 1A).^[31] Aqueous TFA-mediated hydrolysis of the anomeric methyl group and installation of the trifluoro-*N*-phenyl imidate group with Cs₂CO₃ proceeded uneventfully to give donors **1-4**.

For the functionalization on C2 we first investigated the inversion of the C2-triflates **29-32**, generated from the corresponding C2-alcohols **25-28**^[32-35] with a suitable azide or fluoride nucleophile (Scheme 1B).^[36] Inversion of the ribosyl C2-OTf group in **29** using an excess of NaN₃ in DMF at 80°C proceeded smoothly to give the 2-azidoarabinoside **34** high yield (See Table 1, entry 1, conditions A). The inversion of **29** using tetrabutylammonium fluoride (TBAF) as the source of the fluoride nucleophile in THF at ambient temperature gave **38** in good yield (71%, Table 1, entry 2, conditions B). This yield could be further improved to 86% by employing CsF in *tert*-amyl alcohol at 90°C (Table 1, entry 3, conditions C).^[37]



Scheme 1. Reagents and conditions: a) *i.* TEMPO, BAIB, DCM, H₂O; *ii.* MeI, K₂CO₃, DMF; b) TFA/H₂O (9/1); c) 2,2,2-trifluoro-*N*-phenylacetimidoyl chloride, Cs₂CO₃, acetone, H₂O; d) Tf₂O, pyridine, DCM; e) NaN₃, DMF, see Table 1; f) TBAF, THF; or CsF, *tert*-amyl alcohol, see Table 1; g) HCOOH, H₂O; h) 2,2,2-trifluoro-*N*-phenylacetimidoyl chloride, DBU, DCM; i) TFA, H₂O, THF; j) DMAP, DiPEA, thiophosgene, DCM; k) 1,3-dimethyl-2-phenyl-1,3,2-diazaphospholidine, toluene; l) *N*-(phenylseleno)phthalimide, TMSN₃, TBAF, DCM; m) NIS, H₂O, acetone, THF.

Table 1. Synthesis of C2-modified methyl glycosides **33-40** via C2-triflate inversion.

Entry	Triflate	Conditions ^a	Substitution product	Yield (%)	Side products (yield, %)
<i>from D-ribo- to D-arabino-configured</i>					
1	29	A (N ₃)	34	93	-
2	29	B (TBAF)	38	71	-
3	29	C (CsF)	38	86	-
<i>from D-arabino- to D-ribo-configured</i>					
4	30	A	33	86 ^b	51^b
5	30	B	37 , β only	42	30α (17)
6	30	C	37	63	52^f (17)
<i>from D-xylo- to D-lyxo-configured</i>					
7	32α	A ^c	35α	67	53α (12), 55 (7)
8	32α	B ^d	39α	44	28 (17)
9	32α	C ^e	39α	-	54α (57), 55 (21)
10	32β	A ^c	35β	-	53β , (30)
11	32β	B ^d	39β	-	54β (18), 56^g
12	32β	C	39β	-	54β (47), 40β (10)
<i>from D-lyxo- to D-xylo-configured</i>					
13	31	A,B,C	36 / 40	-	56^g

^aReagents and conditions: (A) 0.2 M solution in DMF, 5 eq. NaN₃, 80°C, 2 h; (B) 0.2 M solution in THF, 2.5 eq. TBAF, 0°C to 20°C, overnight; (C) 0.35 M solution in *tert*-amyl alcohol, 4 eq. CsF, 90°C, overnight; ^bCombined yield of **33** and **51**, as a 4:1 mixture. ^cOvernight. ^d70°C, 5 h for entry 8, overnight for entry 11. ^e110°C overnight. ^fα : β = 88 : 12. ^gYield not determined.

When the arabinoside C2 triflate **30** (a mixture of anomers) was treated with conditions A to install the C2 azide and provide **33**, a mixture of products resulted consisting of the desired C2 azide **33** and anomeric azide **51** (Figure 2A; 86%, **33** : **51** = 4 : 1, Table 1, entry 4). Stereospecific formation of β-azide **51** (Figure 2A) can be explained by the generation of a transient methyl oxiranium ion intermediate, that is substituted in an S_N2-like fashion by the azide anion on the anomeric centre (See Figure 2B, path A).^[38]

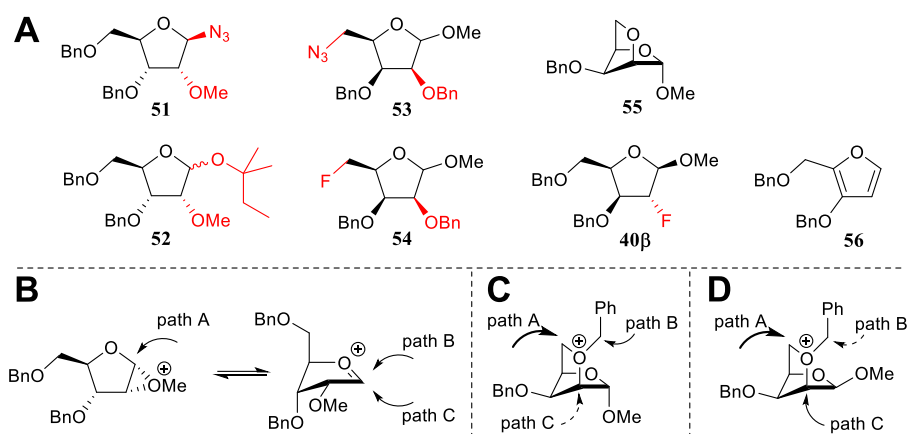


Figure 2. (A) Observed side products **51-56** and **40β**. (B) Proposed reaction pathways for the formation of **51** and **52**. (C) Proposed reaction pathways for the formation of **53α**, **54α** (path A) and **55** (path B). (D) Proposed reaction pathways for the formation of **53β**, **54β** (path A) and **40β** (path C).

The fluoride substitution on **30** also met with side reactions. When **30** was subjected to conditions B, using TBAF, only the β-anomer of **30** reacted to provide **37**, leaving the α-anomer untouched (Table 1, entry 5).^[32] At higher temperatures, using CsF (Conditions C), both anomers reacted to provide the corresponding C2-fluorides. However, reaction of the α-anomer of **30** also provided the anomeric *tert*-amyl product **52** (Figure 2A), resulting from a migration of the anomeric methoxide by substitution of the C2-triflate and subsequent solvolysis of the formed oxocarbenium ion (Figure 2B, path A, B and/or C). The weaker nucleophilicity of *tert*-amyl alcohol with respect to the azide anion likely leads to more S_N1-character in the substitution reaction of the methyl oxiranium ion and generation of an anomeric mixture of **52**, where the azide stereospecifically provided the β-azide **51**.

The xylosyl C2-alcohols **28α** and **28β** could be readily separated and their C2-triflates **32α** and **32β** could therefore be individually investigated in the substitution reactions (Scheme 1B, Table 1, entries 7-12). The inversion of the α-anomer **32α** with NaN₃ provided 2-azidolyxoside **35α** (67%, Table 1, entry 7), alongside two side products, 5-azidolyxoside **53α** and bicycle **55** (Figure 2A), that were formed in 12% and 7% respectively. The generation of these side products stems from the participation of the primary C5-OBn group, which is capable of substituting the C2-OTf. Nucleophilic attack at C5 provides **53α**, while substitution at the benzylic position generates and bicycle **55** (See Figure 2C, path A and B). When the substitution of the C2-triflate **32α** was tried under conditions B to furnish the desired C-2-fluoro lyxose **39α** (Table 1, entry 8), no conversion was observed and therefore the reaction was heated to 70°C. Under these conditions 2-fluorolyxoside **39α** was formed in 44% yield while alcohol **28** was regenerated through hydrolysis of the triflate. Conditions C (Table 1, entry 9) only resulted in the formation of products originating from C5-OBn participation: 5-fluoroxylxoside **54α** and bicycle **55** (Figure 2A and 2D) were obtained in 57% and 21% yield, respectively.

Inversion of the C2-OTf of the β -xyloside **32 β** with either the azide or fluoride nucleophiles did not lead to any desired inversion products (Table 1, entries 10-12). Conditions A only provided the C5-azido product **53 β** (Figure 2A), while conditions B led to the formation of **54 β** , through the participation of the C5-OBn group (Figure 2C, path A). Elimination to give furan **56** was also observed under conditions B (Table 1, entry 11).^[39] Interestingly, the use of CsF (conditions C, Table 1, entry 12) provided, besides sideproduct **54 β** , the 2-fluoroxylsode **40 β** in low yield, apparently through a double displacement mechanism (Figure 2D, path C). Generation of product **40 β** through this route proved advantageous since its generation from *lyxo*-triflate **31** was ineffective (*vide infra*).

All the conditions examined to transform *lyxo*-triflate **31** to one of the inverted products (**36/40**) were ineffective (Table 1, entry 13) and furan **56** was formed exclusively within minutes. We therefore took a different approach to generate the 2-azidoxyloside (Scheme 1C). Thus, glycal **49**^[40] was functionalized by azidophenylselenation with TMSN₃ and *N*-(phenylseleno)phthalimide to give the desired 2-azidoxyloside **50** with good diastereoselectivity (9:1, *xylo:lyxo*).^[41,42] Oxidative hydrolysis of the selenophenyl group by aqueous NIS then gave lactol **44**.

Acidolysis of the anomeric methyl ethers **33-35** and **37-40** using aqueous formic acid provided the other lactols **41-43**, and **45-48** (Scheme 1B). Finally, all eight lactols were transformed into the corresponding *N*-phenyl trifluoroacetimidates **5-12** to complete the set of donor furanosides.

Glycosylations

With the complete set of functionalized furanosyl imidate donors **1-12** in hand, the stereoselectivity of the glycosylation reactions using allyltrimethylsilane (allyl-TMS) or triethylsilane-*d* (TES-*d*) as acceptors, were examined.^[43] Allyl-TMS and TES-*d* are poor nucleophiles and are ideal acceptors to study the S_N1 reaction pathways of the glycosylations at hand.^[15,16,44-46] The results of these glycosylations together with results obtained previously in the tri-*O*-benzyl series (donors **57-60**) are listed in Table 2. As previously described, the reactions in the tri-*O*-benzyl series proceed with good to excellent 1,2-*cis*-selectivity for all four configurations.^[15] The *ribo*-, *arabino*- and *lyxo*-configured donors **57**, **58** and **59** provided exclusively the 1,2-*cis*-substitution products, where the xylose donor **60** gave the anomeric deuterium α - and β -products in a 85:15 α/β -ratio (Table 2, entry 1, 5, 9 and 13). Strikingly, the 1,2-*cis*-selectivity in the glycosylation reactions was also observed for the reactions using the C2- and C5-modified furanosyl donors. All reactions performed with ribose donors **1**, **5** and **9** (Table 2, entries 2-4), arabinose donors **2**, **6** and **10** (entries 6-8), and *lyxo*se donors **3**, **7** and **11** (entries 10-12) proceeded with excellent 1,2-*cis* stereoselectivity. The reactions of the xylose donors **4**, **8**, and **12** (Table 2, entries 14-16) proceed with poorer stereoselectivity. The 2-azidoxyloside donor **8** gives a 85:15 mixture of anomers (product **72**), in line with the outcome of the reaction of the

corresponding tri-*O*-benzyl donor **60** (Table 2, entry 13 and 15). The 2-fluoroxylsides **76** is formed in a 70:30 α : β ratio (Entry 16), and the uronic acid xyloside donor **4** provided the least selective reaction giving roughly equal amounts of both the α - and the β -product (**68**, Table 2, entry 14). The reactions of the xylosyl donors also provided significant quantities of side products. In all reactions, the anomeric *N*-phenyl-trifluoroacetamides (**78-80**, Figure 3) were formed. Although these kind of side products are well known for (pyranosyl) trichloroacetimidate donors,^[47] to our knowledge they have never been reported for the *N*-phenyl trifluoroacetimidates. In the reaction of the xyluronic acid ester **4**, the tricyclic **81** (Figure 3) was also formed, originating from an intramolecular electrophilic aromatic substitution reaction of the C2-*O*-benzyl.

Overall it can be concluded that -quite surprisingly- the nature of the substituents on furanosyl donors has relatively little effect on the stereochemical outcome of the glycosylation reactions.

Table 2. Glycosylation reactions of donors **1-12** and **57-60**, with acceptors TES-*d* and allyl-TMS.

Entry	Donor	Acceptor	Product	1,2- <i>cis</i> : 1,2- <i>trans</i>	Yield (%)
<i>D-ribo-configured</i>					
1	57	TES- <i>d</i>	61	>98 : 2	50 ^a
2	1	allyl-TMS	65	>98 : 2	79
3	5	TES- <i>d</i>	69	>98 : 2	68
4	9	allyl-TMS	73	>98 : 2	76
<i>D-arabino-configured</i>					
5	58	TES- <i>d</i>	62	>98 : 2	62 ^a
6	2	allyl-TMS	66	95 : 5	76
7	6	TES- <i>d</i>	70	>98 : 2	57
8	10	allyl-TMS	74	>98 : 2	79
<i>D-lyxo-configured</i>					
9	59	TES- <i>d</i>	63	>98 : 2	100 ^a
10	3	allyl-TMS	67	>98 : 2	76

11	7	TES- <i>d</i>	71	>98 : 2	59
12	11	allyl-TMS	75	>98 : 2	90
<i>D</i> -xylo-configured					
13	60	TES- <i>d</i>	64	85 : 15	40 ^a
14	4	allyl-TMS	68	45 : 55	57 ^b
15	8	TES- <i>d</i>	72	85 : 15	68 ^b
16	12	allyl-TMS	76	70 : 30	62

Anomeric configuration established by HSQC-HECADE and NOESY NMR.^[48–50] Detailed experimental conditions are provided in the experimental section. ^aLiterature values, see reference 15. ^bCalculated yields from isolated mixed fractions.

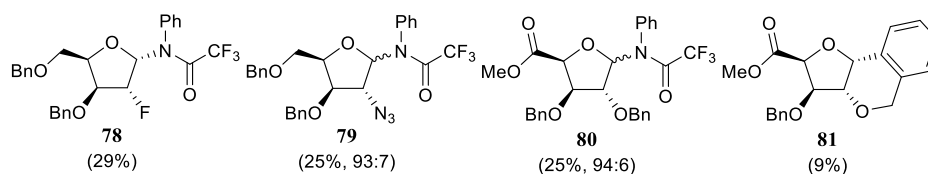


Figure 3. Structures **78–81** identified as side products in the glycosylation reactions of xylosyl imidate donors. Percentages obtained from the crude ¹H NMR.

Computations

To rationalize the stereochemical outcome of the glycosylations described above, we next assessed the structure of the oxocarbenium ions involved. Woerpel and co-workers have devised an empirical model to rationalize the stereoselectivity observed in addition reactions to furanosyl oxocarbenium ions. This model takes the two most relevant structures of the ions, the *E*₃ and ³*E* conformers, into account and describes that these will be preferentially attacked from the ‘inside’ of the envelope (See Figure 4A).^[32,51–54] Thus, the former ion is stereoselectively attacked from the bottom face, while the latter is substituted on the top face and the population of both conformational states determines the overall stereoselectivity. The stereoelectronic effects of the ring substituents dictate the relative stability of the conformers and the stabilizing/destabilizing spatial positions are graphically presented in Figure 4B for the four tri-*O*-benzylfuranosyl oxocarbenium ions. The oxocarbenium ion conformers are most stable when the positive charge at the anomeric centre is stabilized by C2-H hyperconjugation, and by placing the alkoxy substituents at C3 and C5 in an orientation that brings the lone pairs of the oxygen atoms closest to the anomeric centre. In the ribose oxocarbenium ion all substituents can work in concert to stabilize the cation, while in the other three the stabilizing effect of the substituents cannot be matched. For these ions it is difficult to predict what the net effect of the combination of the substituents is and therefore we have developed, based on the initial work of Rhoad and co-workers,^[14] a computational method that maps the relative energy of all possible conformations as a function of their shape. By plotting the energy of the conformers on the pseudo-rotational circle, that is used

to graphically represent all possible 5-ring geometries (Figure 4C),^[55] conformational energy landscape (CEL) maps are created that provide detailed insight into the overall stabilizing/destabilizing effects of the ring substituents in every possible conformation and configuration (See ESI for the full computational method).^[15] These maps can account for the stereoselectivity of addition reactions to fully or partially substituted furanosyl oxocarbenium ions, and the method thus provides an excellent tool to assess the stereoelectronic effects of the functional groups on the ring as a function of their electronic nature and spatial orientation.

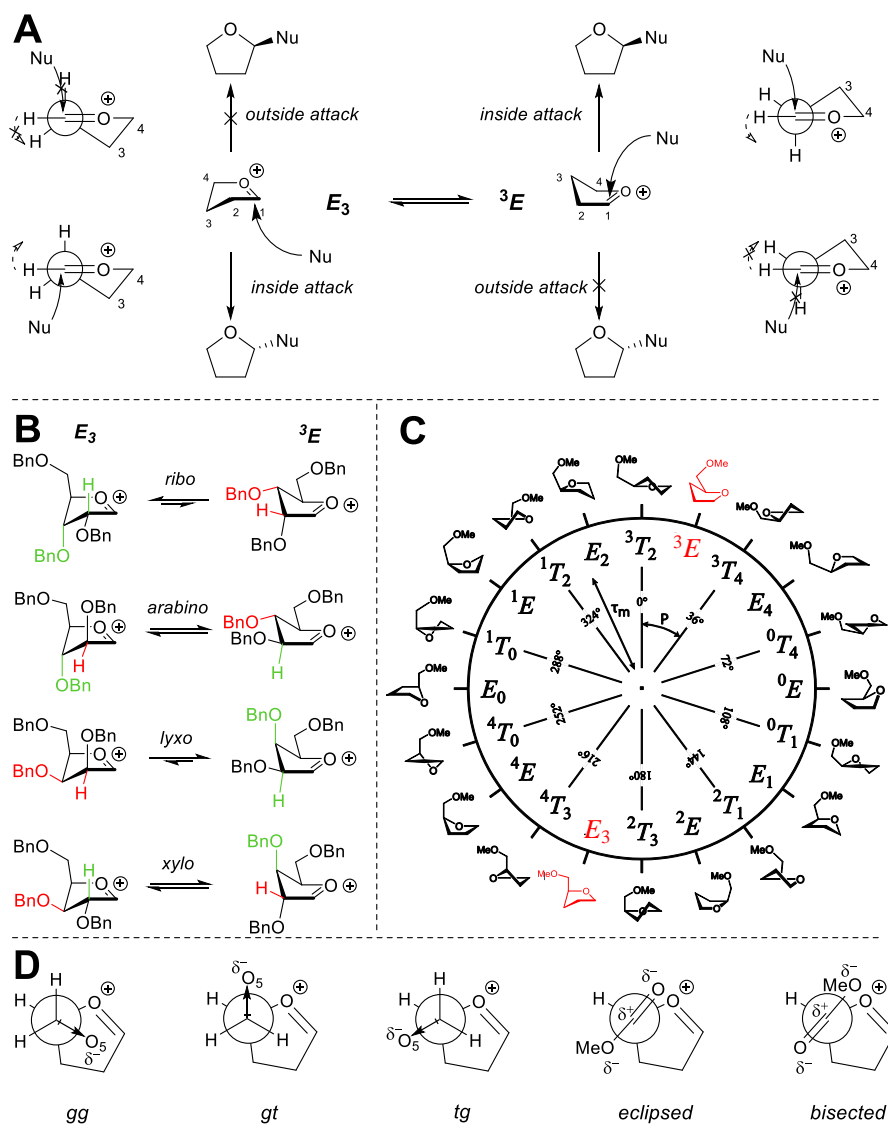


Figure 4. (A) The two-conformer model, visualizing preferential nucleophilic attack from the inside face. Important rotations are denoted by dashed arrows. (B) The two principal conformations of the two-conformer model (E_3 – $3E$) shown for every carbohydrate configuration, examples taken as their tri-*O*-benzyl protected form. Colours indicate relative preferential orientations for H-2 and O-3: green is relatively stabilizing whereas red is relatively destabilizing. (C) Pseudo-rotational circle showing the twenty canonical furanoside structures, with phase-angle P and pucker amplitude τ_m . (D) The possible C4-C5 rotamers: *gg*, *gt*, and *tg* for the C5-OMe oxocarbenium ions, and two rotamers, *eclipsed* and *bisected*, for the C4-CO₂Me oxocarbenium ions.

We therefore adopted this method here to probe the effect of the C2- and C5-modifications on the stability of the oxocarbenium ion conformers and we have calculated the relative energy of the

C4-CO₂Me, C2-N₃ and C2-F furanosyl ions as a function of their shape to deliver the CEL maps shown in Figure 5. To generate these maps the benzyl ethers in the substrates used in the experiments described above have been replaced for methyl ethers (See Figure 5, **82-97**), to minimize computational costs.^[56] For the C2-N₃ and C2-F ions, three maps were generated for each of the C4-C5 *gg*, *gt*, and *tg* rotamers (Figure 4D), and these were combined to provide the overall CEL map shown in Figure 5. A similar approach was taken for the bisected and eclipsed structures of the C4-CO₂Me oxocarbenium ions. The most important conformations for each ion are given next to the CEL map of each oxocarbenium ion in Figure 5 (see ESI for the corresponding energies).

From the CEL maps of the *ribo*-configured furanosyl oxocarbenium ions **82-85** (Figure 5, top row) it becomes clear that the overall shape of the energy landscape is comparable for all four ions, with the energy minima centred on the *E*₃ conformation. This indicates that a fluoride or azide at C2 is best positioned in a *pseudo*-equatorial orientation to allow for stabilization of the ion by hyperconjugation of the C2-H bond, in line with the effect of a C2-ether functionality.^[8,15] From the CEL map of the C2-F ion it does become apparent that there is a stronger tendency of the fluorine atom to occupy a *pseudo*-equatorial orientation. The ³*E* conformer of **85** is 5.2 kcal·mol⁻¹ higher in energy than the lowest energy *E*₃ conformer, whereas this difference is only 1.9 kcal·mol⁻¹ for **82** and around 2.5 kcal·mol⁻¹ for **84**. The preference of the C4-CO₂Me to take up an axial orientation becomes apparent from the CEL map of ion **83**. Interestingly, there is only a marginal difference between the eclipsed and bisected orientation of the carboxylic acid ester and both orientations seem to be equally capable of stabilizing the electron depleted anomeric centre when the C4-CO₂Me takes up a *pseudo*-axial orientation (See ESI). Using the lowest energy *E*₃ conformers as product forming intermediates the formation of the 1,2-*cis* products can be readily accounted for using the inside attack model for all of the examined ribofuranosides.

The CEL maps for *arabino*-configured furanosyl oxocarbenium ions **86-89** (Figure 5, second row) also show great similarity, with each map showing an energy minimum around the ³*E* conformation. Thus, the hyperconjugative stabilization of the C2-H bond, in combination with a sterically favourable *pseudo*-equatorial orientation for all substituents seems decisive for these ions. Inside attack on the ³*E* conformers leads to the formation of the 1,2-*cis*-products as found experimentally. Of note, the C2-N₃ CEL map does show a second energy minimum for the ⁴*T*₃ / ⁴*E* conformer with minimal ring puckering. From the stereochemical outcome of the glycosylation reactions it seems that this conformer does not play a major role in the addition reaction. This could indicate that attack on this almost flat conformer is significantly less favourable than the inside attack of the ³*E* envelope, which leads to the favourable C1-C2 staggered product.

ions. This can be understood by realizing that the E_3 envelope not only loses the stabilizing interactions of the C2 and C3 substituents, present in the 3E conformer, but also experiences severe 1,3-diaxial interactions between the C2 and C4 groups, especially for the electronically most favorable *gg* rotamer. Again, the CEL maps show great similarity for all substitution patterns, indicating analogous behaviour of the lyxofuranosides in glycosylation reaction. This is indeed borne out in the experimental glycosylations that all proceed in an completely stereoselective fashion, to provide the all-*cis* products.

Finally, the *xylo*-configured oxocarbenium ions **94-97** (Figure 5, fourth row) were assessed. Again, the CEL maps of the differently functionalized xylosides appear to be rather similar. Two minima are apparent on either side of the CEL maps. In the low energy E_3 -like structures the C5-OMe groups are positioned in a *gg* orientation to stabilize the electron depleted anomeric centre, while in the low energy 3E -like structures, on the other side of the CEL map, the C5-OMe takes up a *gt* orientation. Notably, the energy minima located on the south side of the CEL maps are relatively broad and not only encompass E_3 -like conformations but also 4T_3 structures, and perhaps more striking, the 4E -like conformers. This latter conformer is in fact the lowest energy species for 2-fluoroxylside **97** and xylosyl uronate **95**, which are the two least selective species (see Table 2). This conformation lacks the stabilizing effect of the O3 electron lone pairs as well as hyperconjugative stabilization by the C2-H bond. Instead, the driving stabilization now appears to be the interaction of the C5-O-methyl or C5 carbonyl that is positioned over the ring in an eclipsed conformation, with the anomeric centre. In the 4E conformation, the steric interactions between C5 and the substituents at C3 and the C2-H are reduced when compared to the sterically unfavourable situation in the E_3 conformer. The established broad energy minima may be at the basis for the poor stereoselectivity observed in the condensations of the xylosyl donors as attack of the 4E conformers may occur from both sides of the ring.

Conclusions

In summary, we have disclosed synthetic routes to access all diastereoisomeric C2-azido and C2-fluoro furanosides as well as all furanosyl uronic acid esters. In total a set of twelve differently functionalized furanosyl donors has been synthesized and these have been glycosylated with allyltrimethylsilane and triethylsilane-*d* to establish the stereoselectivity of these donors in S_N1 -type glycosylation reactions. Exclusive 1,2-*cis*-selectivity was observed for all *ribo*-, *arabino*-, and *lyxo*-configured donors, despite the structural modifications made on the C2- and C5-positions. The 2-azido and 2-fluoro xylose donors were moderately 1,2-*cis*-selective while the xyluronic acid donor reacted in a non-stereoselective manner. The experimental results have been complemented by computational studies, generating Conformational Energy Landscape (CEL) maps for the intermediate oxocarbenium ions. These maps have shown that the stereoelectronic effects of the C2- and C5-modifications are, across the board, similar to an C2-ether substituent. These groups therefore have a similar effect on the stereochemical outcome of glycosylations reactions *taking place*

through an S_N1 -like mechanism and the lowest energy oxocarbenium ion conformers, revealed by the CEL maps have, in combination with the inside attack model, provide a suitable explanation for the experimentally observed *cis*-stereoselectivity. The maps have revealed that for most of the studied furanosyl oxocarbenium ions the canonical 3E and E_3 envelopes represent the lowest energy structures. However, for the xylosyl oxocarbenium ions other low energy structures can be found, taking up 4T_3 and 4E conformations. The occurrence of these structures coincides with relatively poor selectivity in the addition reactions. For these ions it appears that the “two-conformer model” falls short in providing an adequate explanation to account for the (lack of) stereoselectivity and that more oxocarbenium ion conformations have to be taken into account as product forming intermediates. Further insight into the structure of glycosyl oxocarbenium ions and the trajectories of nucleophiles that attack these will lead to a better understanding of the S_N1 -side of the glycosylation reaction mechanism continuum and this can eventually pave the way to new stereoselective glycosylation methodology.^[57]

Acknowledgements

We thank the Netherlands Organization for Scientific Research (NWO) for financial support and the use of supercomputer facilities (SURFsara and the Lisa system) and we kindly acknowledge Mark Somers for technical support.

References

- [1] P. Deslongchamps, *Stereoelectronic Effects in Organic Chemistry*, Pergamon Press, Oxford [Oxfordshire]; New York, **1983**.
- [2] M. Sinnott, *Carbohydrate Chemistry and Biochemistry: Structure and Mechanism*, The Royal Society Of Chemistry, **2007**.
- [3] H. A. Taha, M. R. Richards, T. L. Lowary, *Chem. Rev.* **2013**, *113*, 1851–1876.
- [4] P. O. Adero, H. Amarasekara, P. Wen, L. Bohé, D. Crich, *Chem. Rev.* **2018**, *118*, 8242–8284.
- [5] E. R. van Rijssel, A. P. A. Janssen, A. Males, G. J. Davies, G. A. van der Marel, H. S. Overkleeft, J. D. C. Codée, *ChemBioChem* **2017**, *18*, 1297–1304.
- [6] C. M. Pedersen, M. Bols, *Org. Biomol. Chem.* **2017**, *15*, 1164–1173.
- [7] J. I. Olsen, S. P. A. Sauer, C. M. Pedersen, M. Bols, *Org. Biomol. Chem.* **2015**, *13*, 3116–3121.
- [8] D. M. Smith, K. A. Woerpel, *Org. Biomol. Chem.* **2006**, *4*, 1195–1201.
- [9] H. H. Jensen, M. Bols, *Acc. Chem. Res.* **2006**, *39*, 259–265.
- [10] H. H. Jensen, L. Lyngbye, A. Jensen, M. Bols, *Chem. – Eur. J.* **2002**, *8*, 1218–1226.
- [11] R. J. Woods, C. W. Andrews, J. P. Bowen, *J. Am. Chem. Soc.* **1992**, *114*, 859–864.
- [12] B. Hagen, S. van der Vorm, T. Hansen, V. D. Marel, G. A. J. D. C. Codée, in *Sel. Glycosylations Synth. Methods Catal. Synth. Methods Catal.*, Wiley-VCH Verlag GmbH & Co. KGaA, **2017**, pp. 1–28.
- [13] For selected examples on donor reactivities, see: a) B. Fraser-Reid and J. C. López, in *Reactivity Tuning in Oligosaccharide Assembly*, eds. B. Fraser-Reid and J. Cristóbal López, Springer Berlin Heidelberg, Berlin, Heidelberg, **2011**, pp. 1–29. b) P. Grice, S. V. Ley, J. Pietruszka, H. W. M. Priepe and E. P. E. Walther, *Synlett*, **1995**, *1995*, 781–784. c) N. L. Douglas, S. V. Ley, U. Lücking and S. L. Warriner, *J. Chem. Soc. Perkin 1*, **1998**, 51–66. d) Z. Zhang, I. R. Ollmann, X.-S. Ye, R. Wischnat, T. Baasov and C.-H. Wong, *J. Am. Chem. Soc.*, **1999**, *121*, 734–753. e) K.-K. T. Mong and C.-H. Wong, *Angew. Chem.*, **2002**, *114*,

- 4261–4264. f) C. M. Pedersen, L. G. Marinescu and M. Bols, *Chem. Commun.*, **2008**, 2465–2467. g) M. Heuckendorff, C. M. Pedersen and M. Bols, *J. Org. Chem.*, **2013**, *78*, 7234–7248.
- [14] J. S. Rhoad, B. A. Cagg, P. W. Carver, *J. Phys. Chem. A* **2010**, *114*, 5180–5186.
- [15] E. R. van Rijssel, P. van Delft, G. Lodder, H. S. Overkleeft, G. A. van der Marel, D. V. Filippov, J. D. C. Codée, *Angew. Chem. Int. Ed.* **2014**, *53*, 10381–10385.
- [16] J. M. Madern, T. Hansen, E. R. van Rijssel, H. A. V. Kistemaker, S. van der Vorm, H. S. Overkleeft, G. A. van der Marel, D. V. Filippov, J. D. C. Codée, *J. Org. Chem.* **2019**, *84*, 1218–1227.
- [17] E. R. van Rijssel, P. van Delft, D. V. van Marle, S. M. Bijvoets, G. Lodder, H. S. Overkleeft, G. A. van der Marel, D. V. Filippov, J. D. C. Codée, *J. Org. Chem.* **2015**, *80*, 4553–4565.
- [18] J.-H. Kim, J. Yu, V. Alexander, J. H. Choi, J. Song, H. W. Lee, H. O. Kim, J. Choi, S. K. Lee, L. S. Jeong, *Eur. J. Med. Chem.* **2014**, *83*, 208–225.
- [19] N. M. Evdokimov, P. M. Clark, G. Flores, T. Chai, K. F. Faull, M. E. Phelps, O. N. Witte, M. E. Jung, *J. Med. Chem.* **2015**, *58*, 5538–5547.
- [20] E. A. Weinstein, A. A. Ordonez, V. P. DeMarco, A. M. Murawski, S. Pokkali, E. M. MacDonald, M. Klunk, R. C. Mease, M. G. Pomper, S. K. Jain, *Sci. Transl. Med.* **2014**, *6*, 259ra146-259ra146.
- [21] M. R. Richards, T. L. Lowary, *ChemBioChem* **2009**, *10*, 1920–1938.
- [22] T. L. Lowary, *Acc. Chem. Res.* **2016**, *49*, 1379–1388.
- [23] L. J. van den Bos, J. D. C. Codée, R. E. J. N. Litjens, J. Dinkelaar, H. S. Overkleeft, G. A. van der Marel, *Eur. J. Org. Chem.* **2007**, *2007*, 3963–3976.
- [24] B. Lindberg, in *Adv. Carbohydr. Chem. Biochem.* (Eds.: R.S. Tipson, D. Horton), Academic Press, **1990**, pp. 279–318.
- [25] J. D. C. Codée, A. E. Christina, M. T. C. Walvoort, H. S. Overkleeft, G. A. van der Marel, in *React. Tuning Oligosacch. Assem.* (Eds.: B. Fraser-Reid, J. Cristóbal López), Springer Berlin Heidelberg, Berlin, Heidelberg, **2011**, pp. 253–289.
- [26] In a set of preliminary glycosylations the anomeric acetates of the C2- and C5-modified glycosides were discarded as donors since they were unreactive even at room temperature, by nature of their electron-withdrawing substituents. The tri-*O*-benzyl furanoside donors were converted to trifluoro-*N*-phenylacetimidates and reacted at -78°C with allyltrimethylsilane. Analysis of the crude product samples by ¹H NMR revealed the same stereochemistry as reported in Table 1, acetyl donors **57-60**, deuterated products **61.64**. A sample of the unknown 1-allyl-2,3,5-tri-*O*-benzyl 1-deoxy-lyxofuranoside is reported in the ESI (**77**).
- [27] P. A. Wender, F. C. Bi, N. Buschmann, F. Gosselin, C. Kan, J.-M. Kee, H. Ohmura, *Org. Lett.* **2006**, *8*, 5373–5376.
- [28] A. N. Cuzzupe, R. Di Florio, M. A. Rizzacasa, *J. Org. Chem.* **2002**, *67*, 4392–4398.
- [29] G. H. Veeneman, L. J. F. Gomes, J. H. van Boom, *Tetrahedron* **1989**, *45*, 7433–7448.
- [30] K.-Y. Li, J. Jiang, M. D. Witte, W. W. Kallemeijn, H. van den Elst, C.-S. Wong, S. D. Chander, S. Hoogendoorn, T. J. M. Beenakker, J. D. C. Codée, et al., *Eur. J. Org. Chem.* **2014**, *2014*, 6030–6043.
- [31] L. J. van den Bos, J. D. C. Codée, J. C. van der Toorn, T. J. Boltje, J. H. van Boom, H. S. Overkleeft, G. A. van der Marel, *Org. Lett.* **2004**, *6*, 2165–2168.
- [32] C. H. Larsen, B. H. Ridgway, J. T. Shaw, D. M. Smith, K. A. Woerpel, *J. Am. Chem. Soc.* **2005**, *127*, 10879–10884.
- [33] C. Jia, Y. Zhang, L.-H. Zhang, P. Sinaÿ, M. Sollogoub, *Carbohydr. Res.* **2006**, *341*, 2135–2144.
- [34] V. Popsavin, S. Grabež, B. Stojanović, M. Popsavin, V. Pejanović, D. Miljković, *Carbohydr. Res.* **1999**, *321*, 110–115.
- [35] T. K. Chakraborty, D. Koley, R. Ravi, V. Krishnakumari, R. Nagaraj, A. Chand Kunwar, *J. Org. Chem.* **2008**, *73*, 8731–8744.
- [36] K. J. Hale, L. Hough, S. Manaviazar, A. Calabrese, *Org. Lett.* **2015**, *17*, 1738–1741.

- [37] O.-M. Soueidan, B. J. Trayner, T. N. Grant, J. R. Henderson, F. Wuest, F. G. West, C. I. Cheeseman, *Org. Biomol. Chem.* **2015**, *13*, 6511–6521.
- [38] K. C. Nicolaou, T. Ladduwahetty, J. L. Randall, A. Chucholowski, *J. Am. Chem. Soc.* **1986**, *108*, 2466–2467.
- [39] T.-L. Su, R. S. Klein, J. J. Fox, *J. Org. Chem.* **1981**, *46*, 1790–1792.
- [40] R. R. Diaz, C. Rodríguez Melgarejo, I. I. Cubero, M. T. Plaza López-Espinosa, *Carbohydr. Res.* **1997**, *300*, 375–380.
- [41] R. Hernández, E. I. León, P. Moreno, C. Riesco-Fagundo, E. Suárez, *J. Org. Chem.* **2004**, *69*, 8437–8444.
- [42] S. Czernecki, E. Ayadi, D. Randriamandimby, *J. Org. Chem.* **1994**, *59*, 8256–8260.
- [43] Allylations with allyltrimethylsilane were preferred over reductions with triethylsilane-*d*, as the allyl glycosides were easier to purify, gave higher yields and easier to identify their anomeric configuration.
- [44] S. van der Vorm, T. Hansen, H. S. Overkleeft, G. A. van der Marel, J. D. C. Codee, *Chem. Sci.* **2017**, *8*, 1867–1875.
- [45] J. R. Krumper, W. A. Salamant, K. A. Woerpel, *Org. Lett.* **2008**, *10*, 4907–4910.
- [46] J. R. Krumper, W. A. Salamant, K. A. Woerpel, *J. Org. Chem.* **2009**, *74*, 8039–8050.
- [47] H. M. Christensen, S. Oscarson, H. H. Jensen, *Carbohydr. Res.* **2015**, *408*, 51–95.
- [48] J. G. Napolitano, J. A. Gavín, C. García, M. Norte, J. J. Fernández, A. Hernández Daranas, *Chem. – Eur. J.* **2011**, *17*, 6338–6347.
- [49] W. Koźmiński, D. Nanz, *J. Magn. Reson.* **1997**, *124*, 383–392.
- [50] B. L. Marquez, W. H. Gerwick, R. T. Williamson, *Magn. Reson. Chem.* **2001**, *39*, 499–530.
- [51] J. T. Shaw, K. A. Woerpel, *J. Org. Chem.* **1997**, *62*, 6706–6707.
- [52] J. T. Shaw, K. A. Woerpel, *Tetrahedron* **1999**, *55*, 8747–8756.
- [53] C. H. Larsen, B. H. Ridgway, J. T. Shaw, K. A. Woerpel, *J. Am. Chem. Soc.* **1999**, *121*, 12208–12209.
- [54] T. J. Bear, J. T. Shaw, K. A. Woerpel, *J. Org. Chem.* **2002**, *67*, 2056–2064.
- [55] C. Altona, M. Sundaralingam, *J. Am. Chem. Soc.* **1972**, *94*, 8205–8212.
- [56] Benzyl ethers and methyl ethers behave similarly in glycosylation leading to similar stereoselectivity. See for example: M. G. Beaver, K. A. Woerpel, *J. Org. Chem.* **2010**, *75*, 1107–1118 and Reference 15.
- [57] L. Zhang, K. Shen, H. A. Taha, T. L. Lowary, *J. Org. Chem.* **2018**, *83*, 7659–7671.

Table of Contents Graphic

